JOURNAL OF VIROLOGY, Aug. 1995, p. 4994–5010 Vol. 69, No. 8
0022-538X/95/$04.00+0

Egress of Varicella-Zoster Virus from the Melanoma Cell: a Tropism for the Melanocyte

ROBERT HARSON AND CHARLES GROSE*

Department of Microbiology, University of Iowa College of Medicine, Iowa City, Iowa 52242

Received 8 March 1995/Accepted 10 May 1995

The pathway of envelopment and egress of the varicella-zoster virus (VZV) and the primary site of viral production within the epidermal layer of the skin are not fully understood. There are several hypotheses to explain how the virus may receive an envelope as it travels to the surface of the monolayer. In this study, we expand earlier reports and provide a more detailed explanation of the growth of VZV in human melanoma cells. Human melanoma cells were selected because they are a malignant derivative of the melanocyte, the melanin-producing cell which originates in the neural crest. We were able to observe the cytopathic effects of syncytial formation and the pattern of egress of virions at the surfaces of infected monolayers by scanning electron microscopy and laser-scanning confocal microscopy. The egressed virions did not appear uniformly over the syncytial surface, rather they were present in elongated patterns which were designated viral highways. In order to document the pathway by which VZV travels from the host cell nucleus to the outer cell membrane, melanoma cells were infected and then processed for examination by transmission electron microscopy (TEM) at increasing intervals postinfection. At the early time points, within minutes to hours postinfection, it was not possible to localize the input virus by TEM. Thus, viral particles first observed at 24 h postinfection were considered progeny virus. On the basis of the TEM observations, the following sequence of events was considered most likely. Nucleocapsids passed through the inner nuclear membrane and acquired an envelope, after which they were seen in the endoplasmic reticulum. Enveloped virions within vacuoles derived from the endoplasmic reticulum passed into the cytoplasm. Thereafter, vacuoles containing nascent enveloped particles acquired viral glycoproteins by fusion with vesicles derived from the Golgi. The vacuoles containing virions fused with the outer plasma membrane and the particles appeared on the surface of the infected cell. Late in infection, enveloped virions were also present within the nuclei of infected cells; the most likely mechanism was retrograde flow from the perinuclear space back into the nucleus. Thus, this study suggests a role for the melanocyte in the pathogenesis of VZV infection, because all steps in viral egress can be accounted for if VZV subsumes the cellular pathways required for melanogenesis.

Varicella-zoster virus (VZV) is a member of the *Herpesviridae* family. The 125-kbp genome, smallest of all human herpesviruses, is enclosed in an icosahedral nucleocapsid (7). The viral nucleocapsid is surrounded by a tegument and a lipid envelope. Nucleocapsids are assembled in the nucleus of the host cell. The means by which herpesviruses travel from the nucleus to the outer cell membrane has been the subject of speculation for more than 30 years. As part of a continuing investigation, we have studied egress of VZV by a combination of methods, including transmission electron microscopy (TEM), scanning electron microscopy (SEM), and most recently laser-scanning confocal microscopy.

In previous reports by this laboratory, we have investigated the egress of VZV. In one study, we combined TEM with autoradiography and showed in a series of timed experiments that viral fucosylated glycoproteins were transported from the Golgi/trans-Golgi network into virion-laden cytoplasmic vacuoles (16). In turn, the cytoplasmic vacuoles traveled to the outer cell membrane, after which the viral particles were observed on the cell surface. In that study it was suggested that envelopment by viral glycoproteins occurred within cytoplasmic vacuoles. In a second report, we showed that viral particles could be visualized on the surface of an infected cell by SEM (27). This observation was surprising because the cell-associated nature of VZV infection led to the assumption that viral particles may not be easily observed on the surface of an infected cell. In spite of the above observations, mainly during late infection, we had not yet determined a time course for the egress of virions or the formation of cell-to-cell fusion in human melanoma cells. Furthermore, there remained portions of the viral cycle of egress which were unclear; namely, the method by which the nucleocapsid exits the nucleus and the means by which the cytoplasmic vacuoles are formed. Therefore, in this report we reexamine the entire route of VZV egress from the nucleus to the outer cell membrane. We also demonstrate that enveloped virions are found within the nuclei of infected cells at time points late in infection.

Finally, we present a new hypothesis regarding the location of VZV virion assembly. We propose that the melanocyte is a site of viral replication and transport in the human host prior to the appearance of viral particles in the typical vesicular lesions of chickenpox. Of great interest, this same hypothesis may explain the selective replication of Marek's disease virus (MDV) in the feather follicles of chickens.

MATERIALS AND METHODS

Virus and cell culture. The cell substrate for all experiments was a human melanoma cell line designated MeWo (13). The source of virus was the VZV-32 strain, which is a low-passage virus (less than passage 20) originally isolated from a child with chickenpox (12). For the SEM and TEM experiments, the cells were grown in 35-mm-diameter tissue culture dishes. When the cells had reached near confluency, they were inoculated with VZV-infected cells at a ratio of one infected cell to eight uninfected cells. The cultures were then incubated at 32°C for various times (12). When the monolayers were harvested, they were fixed with 2.5% glutaraldehyde in 0.1 M sodium cacodylate buffer, pH 7.2.

* Corresponding author. Mailing address: University Hospital/2501 JCP, 200 Hawkins Dr., Iowa City, IA 52242. Fax: (319) 356-4855.

SEM sample preparation. After 1 h, the fixative was removed. The sample was rinsed three times with a 0.1 M sodium cacodylate buffer, pH 7.2. The sample was then postfixed with 1% OsO_4 solution. The osmium solution was removed, and the sample was again rinsed three times with 0.1 M sodium cacodylate buffer, pH 7.2. The sample was rinsed briefly in double-distilled H_2O and then dehydrated by using successively higher concentrations of ethanol (EtOH). Following dehydration with 100% EtOH, hexamethyldisilazane (HMDS) was added. After removal of HMDS, the sample was allowed to air dry (14).

When dry, the monolayer was excised from the tissue culture dish. The disc was then mounted to an aluminum stub, and the edges were painted with a silver colloid. When the colloid dried, the sample was sputter coated with a gold palladium alloy. Following sputter coating, the samples were viewed with a Hitachi S-4000 scanning electron microscope (Hitachi Instruments, Inc., Mito City, Japan).

TEM specimen preparation. Following 1 h of fixation with 2.5% glutaraldehyde, the sample was washed three times with 0.1 M sodium cacodylate. The buffer was then removed, and a 1% OsO_4 solution was added for 30 min. After 30 min, the osmium solution was removed and the sample was again rinsed with the buffer. The buffer was removed, and the sample was rinsed for 1 min with double-distilled H_2O. The water was removed, and the sample was en bloc stained with 2.5% uranyl acetate (UA) for 5 min. After the UA step, the sample was dehydrated with successively higher concentrations of EtOH. After the sample had been dehydrated with 100% EtOH, a 1:1 mixture of Eponate-12 resin (Ted Pella, Inc.) and 100% EtOH was added to the samples for 30 min. The mixture was removed, and 100% resin was added for 30 min. The resin was changed two more times; after the second time the sample was placed in a dry bath at 45°C overnight. The temperature was raised to 65°C for an additional 24 h; then the sample was removed from the plastic tissue culture dish (14). An important difference between this set of TEM experiments and the majority of previously reported TEM experiments with cell culture is that the monolayers were not dislodged from the culture dish prior to embedment. Rather, the intact monolayer was embedded directly on the tissue culture dish. The resin containing the embedded monolayer was subsequently separated from the tissue culture dish. This alteration in the protocol allowed for consistency in the orientation of the monolayers throughout the experiments. This protocol was followed also in experiments with laser-scanning confocal microscopy.

The sample was then mounted onto a resin post and cut into thin sections with a Reichert Ultracut E ultramicrotome (Reichert-Jung, Vienna, Austria). Sections were cut in cross section as well as en face. The samples were placed on copper grids and stained with UA and Reynold's lead citrate (26, 33). After being stained, the samples were viewed with a Hitachi H-7000 transmission electron microscope (Hitachi Instruments).

Confocal microscopy and immunocytochemistry. The MeWo cells were grown to confluency in Lab-Tek chamber slides (model 177429). The cells were inoculated with virus-infected cells. The cells exhibited 100% cytopathic effect (CPE) by 72 h postinfection. In order to allow the primary and secondary antibodies to enter the cells, it was necessary to permeabilize the cell membranes with a solution of fresh 2% paraformaldehyde, 0.01 M phosphate-buffered sodium chloride (PBS), pH 7.4, and 0.05% Triton. Samples were blocked with 5% normal goat serum in PBS prior to the addition of primary antibody. The probe was monoclonal antibody 3B3 (20). The primary antibody was incubated on the monolayer overnight. The goat anti-mouse secondary antibody was conjugated with fluorescein isothiocyanate (Molecular Probes, Inc.). After 60 min, the secondary antibody was removed and the samples were again rinsed with PBS. The chambers were removed from the slides, and 1 to 2 drops of Vectashield (Vector Laboratories, Inc.) were added to the samples (25). A large glass coverslip was placed over the samples, and the samples were viewed with a BioRad MRC 600 laser-scanning confocal microscope (BioRad, Cambridge, Mass.) equipped with a krypton/argon laser mounted on a Nikon Optiphot. Images were stored on an optical disc for subsequent viewing.

RESULTS

Topography of an infected cell monolayer. VZV is strongly cell associated. Free viral particles are rarely detected in the culture medium overlying infected cells (35). Infectivity can best be transferred in vitro by passage of trypsin-dispersed inoculum cells that are infected with VZV. The multiplicity of infection is difficult to regulate because inoculum cells contain an indeterminate number of viral particles, but in general we have obtained inocula from infected MeWo monolayers with 75% CPE, as previously described by this laboratory (12, 13).

MeWo cells that had been infected with VZV were viewed by SEM. SEM provides excellent resolution of cellular surface structure. A viral particle of 200 nm can easily be seen by this technique. The most obvious consequences of VZV infection observed through SEM included syncytium formation and the presence of viral particles on the surfaces of the monolayers. In a previous report (27), we showed that viral particles were easily visualized by SEM on the infected cell surface late in infection, but we had not yet determined a precise time course by SEM observation. Because of the requirements for different levels of magnification by SEM, the development of cytopathologic changes over time is shown in Fig. 1, and the appearance of viral particles at increasing intervals postinfection is shown in Fig. 2. Although the time frame involved with these CPEs was somewhat variable, depending on the confluency of monolayers and the size of the inoculum, the sequence of events was entirely predictable from experiment to experiment.

Replicate monolayers inoculated with VZV-infected cells were harvested at increasing intervals following infection. Time points ranged from 15 min to 72 h postinfection; usually there were six time points per experiment. The complete time course experiment was repeated five times. In the initial stages, 15 to 30 min after infection, clusters of inoculum cells were rounded and rested on the surface of the monolayer. The inoculum cells often were connected to one another by long filamentous cellular strands. At this early stage of infection, there were no visible signs of cytopathology and viral particles were not detected on either the inoculum cells or the newly infected monolayer.

At 8 h postinfection there were no visible signs of CPE. The surface of the monolayer contained blebs and microvilli. These surface structures were present on all cells and can easily be seen in Fig. 2A to C. Of note, the number of microvilli appeared to increase in later stages of infection. An occasional viral particle was detected at these early time points. The monolayers that were harvested at the 20-h time point looked very similar to those from the 8-h time point. Syncytium formation was not evident, and viral particles were rarely seen on the surface of the monolayer. The sporadic viral particles seen on the cell surface within the first 24 h postinfection most likely represented nascent virions emerging from the infected cell inoculum. This conclusion is based on the fact that enveloped viral particles were rarely seen within the infected cell by TEM in the first 24 h postinfection (see below).

At 30 h postinfection early fusion was apparent in the monolayer. The fusion was localized to small foci throughout the monolayer. Viral particles on the surfaces of the monolayers became more evident, but large areas of viral egress were still not seen. Of importance, viral particles only appeared within areas of syncytial formation. This observation further supported the conclusion that the sparse particles seen earlier were included within the inoculum.

The foci of cellular fusion in the monolayers that were harvested at 50 h postinfection were much larger. These syncytia represented hundreds of fused cells. Viral particles were present in small, elongated clusters overlying the syncytia. Most particles were around 200 nm in diameter or somewhat larger. The infected cells were completely fused at 70 h postinfection. In other words, the entire monolayer appeared to represent one syncytium. Under low SEM magnification, long diagonal lines were seen across the surface of the syncytia (Fig. 1F). These pathways actually represent thousands of viral particles. The elongated clusters of emerging viral particles have been designated viral highways. Figure 2F is a 15,000× magnification of an area of viral egress within a viral highway. Some of the viral particles lacked a nucleocapsid and appeared doughnut shaped. These structures may correspond to the so-called light particles (31); however, on the basis of the extensive TEM examination of cytoplasmic particles described below, they most likely represented envelopes from which the nucleocapsid has been expelled during the fixation process.

Viral highways and viral syncytia. The viral highways men-

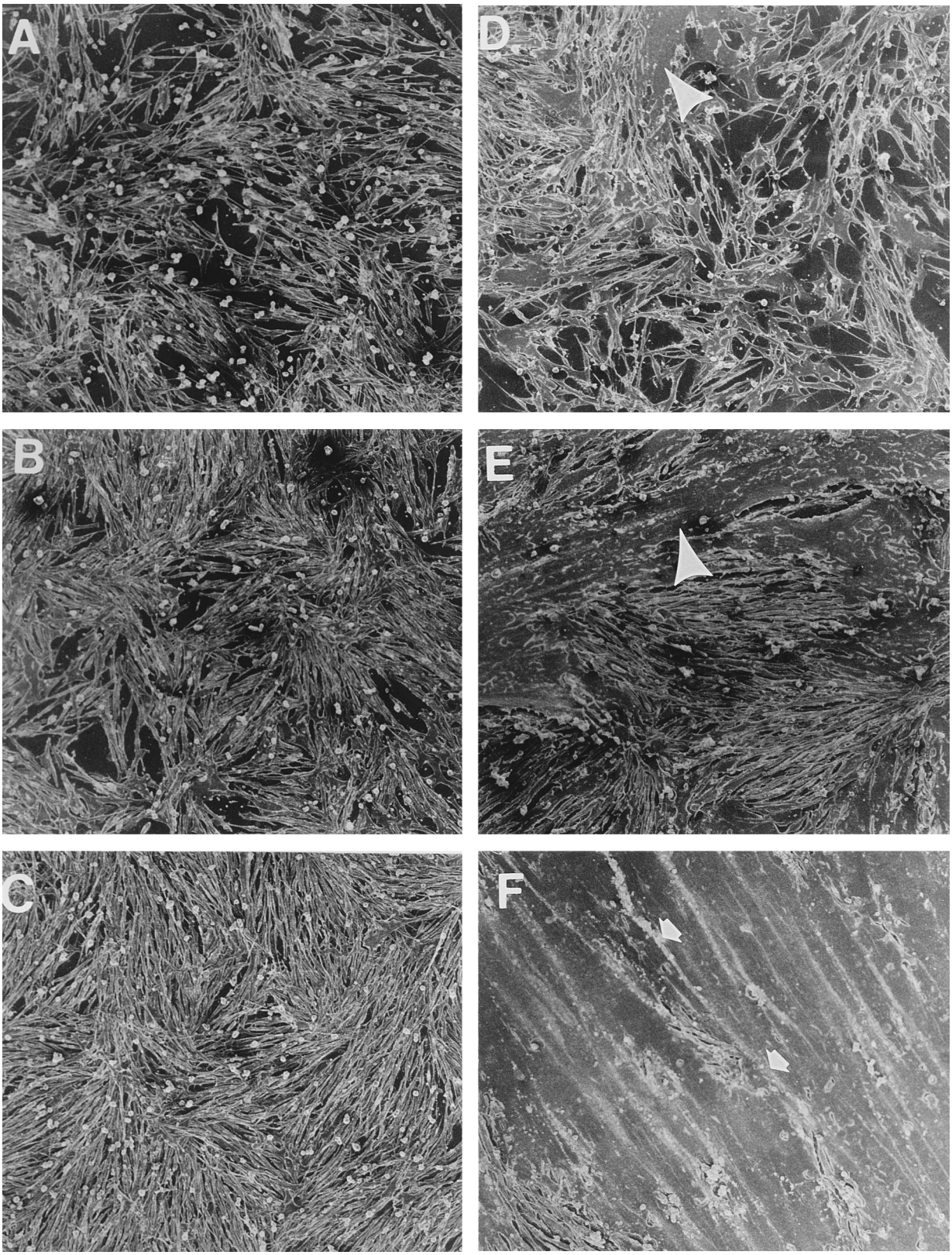

FIG. 1. VZV syncytium formation viewed by SEM. (A) VZV-infected MeWo cells at 30 min postinfection. SEM revealed no evidence of cellular fusion in the monolayer. Inoculum cells were seen as rounded cells on the surface of the monolayer. This micrograph and others below were taken at a magnification of 100×. (B) At 8 h postinfection, the monolayer remained intact with no recognizable signs of CPE. (C) At 20 h postinfection, syncytia were not detectable. (D) At 30 h postinfection, the monolayers developed small foci of syncytium formation (arrowhead). (E) At 50 h postinfection, the foci increased in size and the large syncytia included hundreds of fused cells (arrowhead). (F) At 70 h postinfection, the infected cells were completely fused into one large syncytium. Note the diagonal white lines which are described in more detail in Fig. 2, 3A, and 4 (arrowheads).

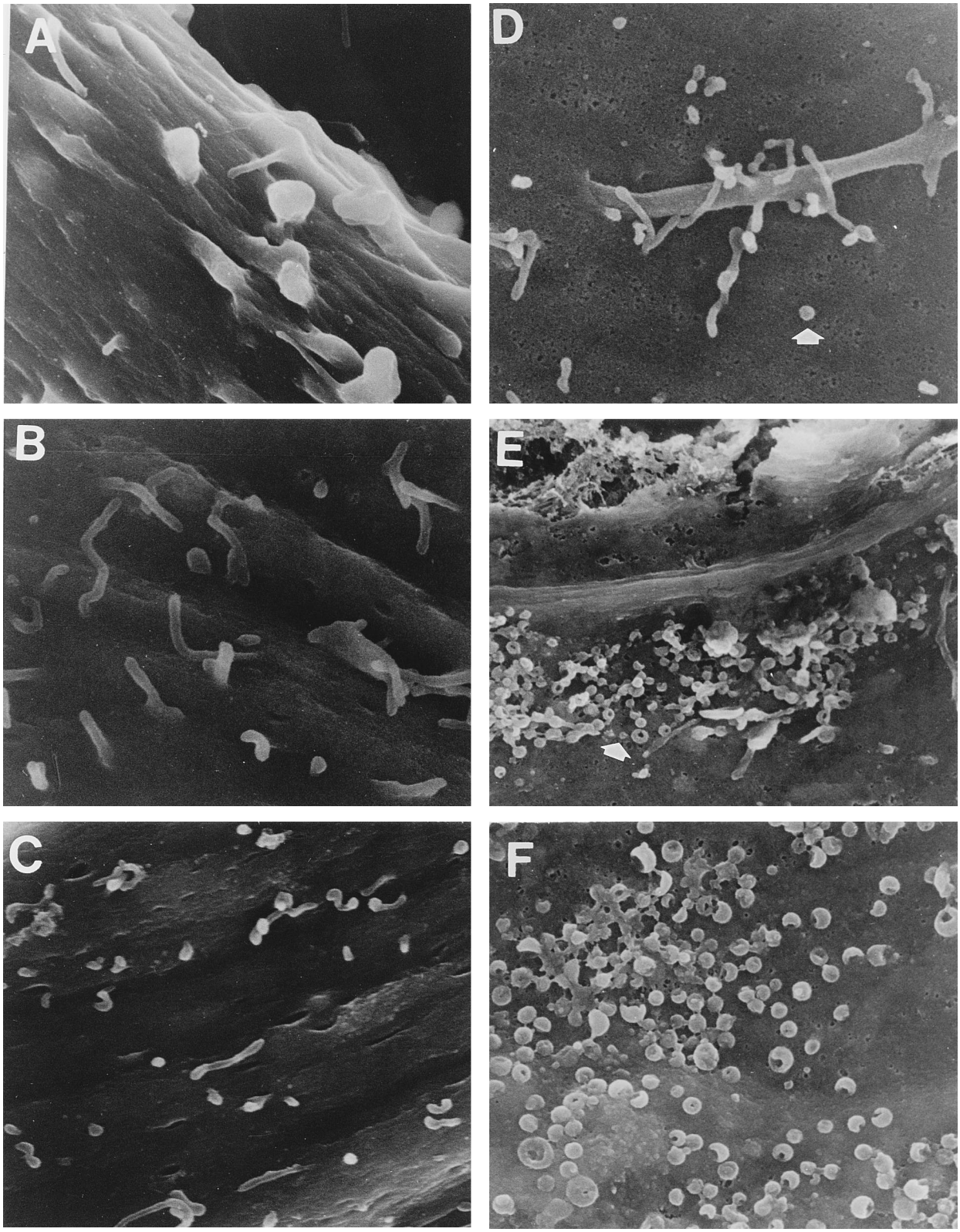

FIG. 2. Egress of VZV particles from melanoma cells. (A) VZV-infected MeWo cells at 30 min postinfection. The surfaces of the cells contained blebs and microvilli, but no viral particles were detected by SEM. All micrographs in this figure were taken at a magnification of 15,000×. (B) At 8 h postinfection, there were no signs of viral egress on the surface of the monolayer. (C) At 20 h postinfection, an occasional viral particle was seen on the surface of the monolayer. The cells also had microvilli and blebs similar to the cells in panels A and B. (D) At 30 h postinfection, more viral particles were visible on the surface of the monolayer, but their numbers were still limited (arrowhead). (E) At 50 h postinfection, the viral particles were readily apparent on the surface of the monolayer (arrowhead). Some of these viral particles were doughnut shaped and appeared to be devoid of a nucleocapsid. (F) At 70 h postinfection, hundreds of viral particles were present throughout the monolayer. Most were concentrated over large syncytia. Several examples of the aberrant doughnut-shaped particles were evident.

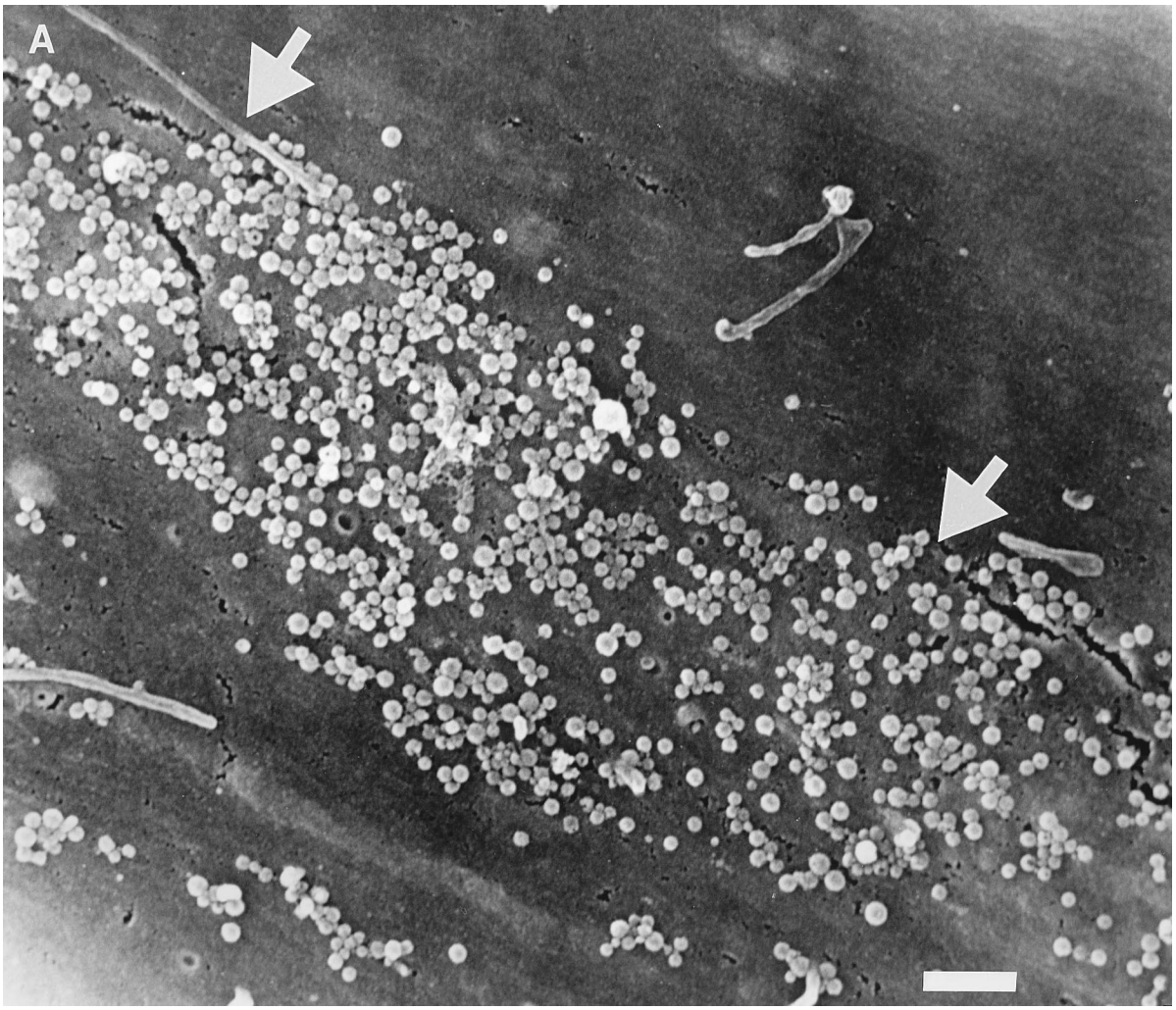

FIG. 3. Syncytium formed by VZV infection. (A) Surface of VZV syncytium. When viewed by SEM late in infection, the entire monolayer was a syncytium with no discernible cellular boundaries. Egressed virions were visible on the surface. They were distributed in an elongated pattern termed viral highways (arrows). Bar, 1 μm. (B) Interior of VZV syncytium. When viewed by TEM, more than 20 nuclei (N) were seen within a syncytium late in infection. The nuclei were not separated by a cytoplasmic membrane, so they represented a true polykaryon. Bar, 5 μm.

tioned above were a phenomenon of late infection of MeWo cells with VZV. The rows of viral particles began to form above syncytia on day 2 and were most evident on day 3 postinfection. Figure 3A shows a representative SEM example of this peculiar arrangement of egressed viral particles. The infected cells were completely fused at this time point, so no individual melanoma cells were detected. The viral particles are present along diagonal rows in the micrograph. Hundreds of individual particles were clearly visualized upon the surface of the monolayer, along with scattered microvilli.

Syncytia are formed by the action of viral fusogens, including viral glycoproteins (28). As the cell membranes fused postinfection, individual nuclei congregated together and polykaryocytosis was evident within the VZV-infected cell monolayer. The arrangement of the nuclei in a large syncytia was visualized by TEM. Figure 3B shows more than 20 nuclei arranged adjacent to one another, with cytoplasm lying to the exterior of the nuclear cluster. This photograph demonstrated conclusively that multiple cells were fused, with no membranes separating one nucleus from another. Several of the nuclei contained an electron-dense inclusion body, as well as areas of condensed chromatin around the interior of the nucleus. The cytoplasm was filled with mitochondria and endoplasmic reticulum (ER), but few Golgi were seen in this section. Nucleocapsids were evident within this micrograph as small solid circles inside of the nucleus.

Immunodetection of viral highways and polykaryocytosis. Syncytia and viral highways were also visualized with laser-scanning confocal microscopy. Confocal microscopy was chosen over the traditional light microscope because of its increased resolution in the *z*-axis plane and the advantages of an electronic image (25). The images were stored electronically on an optical disc and were enhanced to increase contrast. The electronic images were also enhanced with pseudocolor which emphasized ultrastructural detail. Whole-mount tissue-cultured cells were visualized as optical sections with this technique. This method is an advantage over the tedious thin sectioning required for viewing samples with the transmission electron microscope.

The micrographs in Fig. 4 were labeled with antibody against VZV gE (formerly called gpI). In panel A, the viral highways were detected easily on the surfaces of the syncytia; they ap-

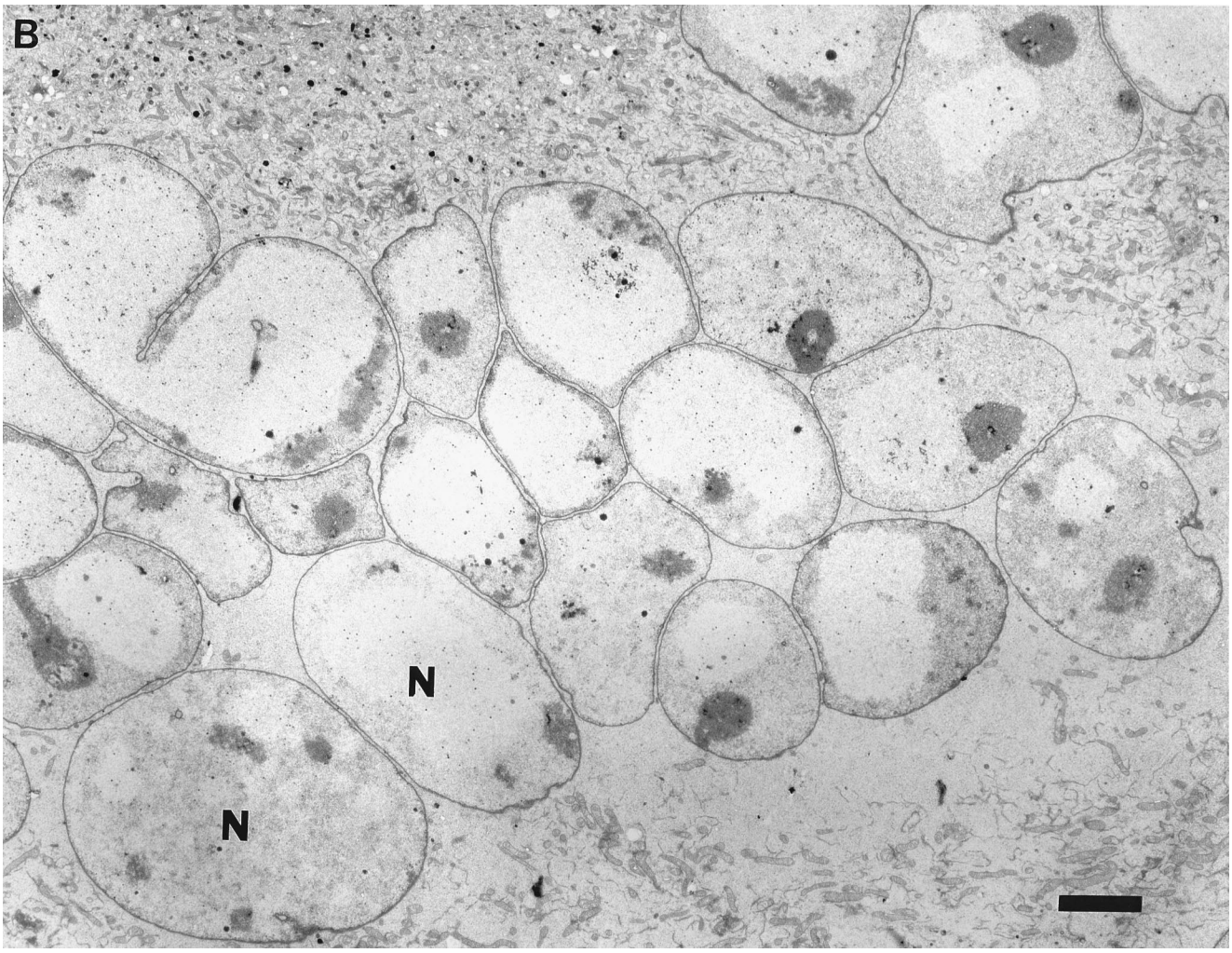

FIG. 3—*Continued.*

peared as whitish lines across the monolayer. The color white indicates the high intensity of labeling of gE, which is the preponderant glycoprotein of the VZV virion (20). Thus, this experiment confirmed our prior data that the particles observed on the surface of the monolayer contained viral glycoproteins (10). Clusters of nuclei in the fused monolayer were seen as dark circles. There was no labeling of VZV gE in these areas, as would be expected because gE is produced within the Golgi apparatus. Because the anti-VZV gE antibody probe could enter the cell and attach to the nascent glycoproteins as they traversed through the cytoplasm, polykaryocytosis was clearly demonstrated in a VZV-infected cell monolayer. The nuclei within the syncytium in Fig. 4B maintained their integrity following the fusion of the cells in which these nuclei were originally located. The 3B3 antibody is an ideal reagent for these studies because it binds a linear epitope extremely resistant to denaturation (20).

Nucleocapsids in the nucleus. SEM revealed many of the cell surface phenomena associated with VZV infection. The TEM exposed the interior of the cell and allowed for a better understanding of the mechanics of viral infection. First of all, we examined multiple samples which were collected from monolayers between 1 and 24 h postinfection. Viral particles were rarely detectable in these samples, either in the cytoplasm or nucleus. Thus, inoculum virus was exceedingly difficult to document by TEM in the newly infected cells, presumably because the numbers were too small. Between 24 and 48 h postinfection, nucleocapsids were first detected in the nucleus; from 48 to 72 h, they greatly increased in number. The panels in Fig. 5 illustrate the appearance of nucleocapsids in the nucleus and their eventual egress. These nucleocapsids were present individually and in small clusters within the nucleoplasm; for example, Fig. 5B shows a nearly crystalline cluster of over 20 nucleocapsids. The emergence of viral particles through the inner nuclear membrane is shown in panels C and D. In panel C, the inner nuclear membrane shows a slight indentation, while in panel D the particle is nearly surrounded by the inner nuclear membrane. In Fig. 5E, the particle, which now contains an envelope, is clearly situated within the perinuclear space and the outer nuclear membrane is pushed outward. Also in Fig. 5E, note the obvious difference in size between the particle still in the nucleoplasm and the particle between the nuclear membranes. In Fig. 5F, the same particles are contained within vacuoles which appear contiguous with the outer nuclear membrane and presumably represent the smooth endoplasmic reticulum (SER). Again, note the difference in size between the particles still in the nucleus compared with those in the vacuoles. The reason we have speculated that

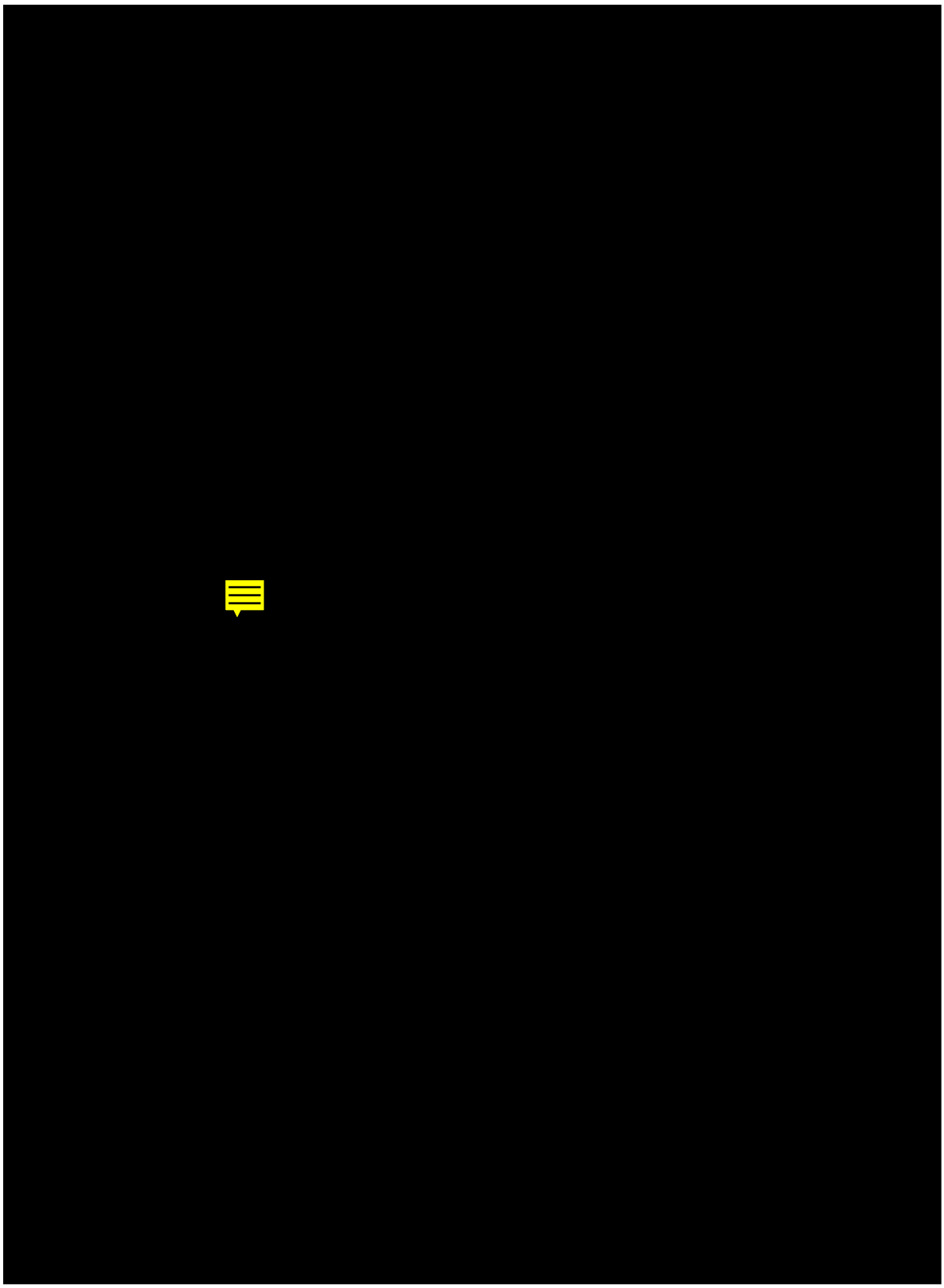

FIG. 4. Viral highways. Laser-scanning confocal microscopy was performed on VZV-infected cell cultures. The probe was monoclonal antibody 3B3 which detects VZV gE (formerly gpI). (A) Viral highways were delineated by the white colored lines across the surface of the infected monolayer. The viral glycoprotein was concentrated in the envelopes of emergent virions (arrows). Bar, 25 μm. (B) Polykaryocytosis was detected within a VZV-induced syncytium. The viral glycoprotein was present in large quantity in the cytoplasm since it is produced in the Golgi and then transported to the cell surface. The nuclei which lack staining were outlined (arrows). Since this serial section was below the surface of the monolayer, viral highways were not visible. Bar, 25 μm.

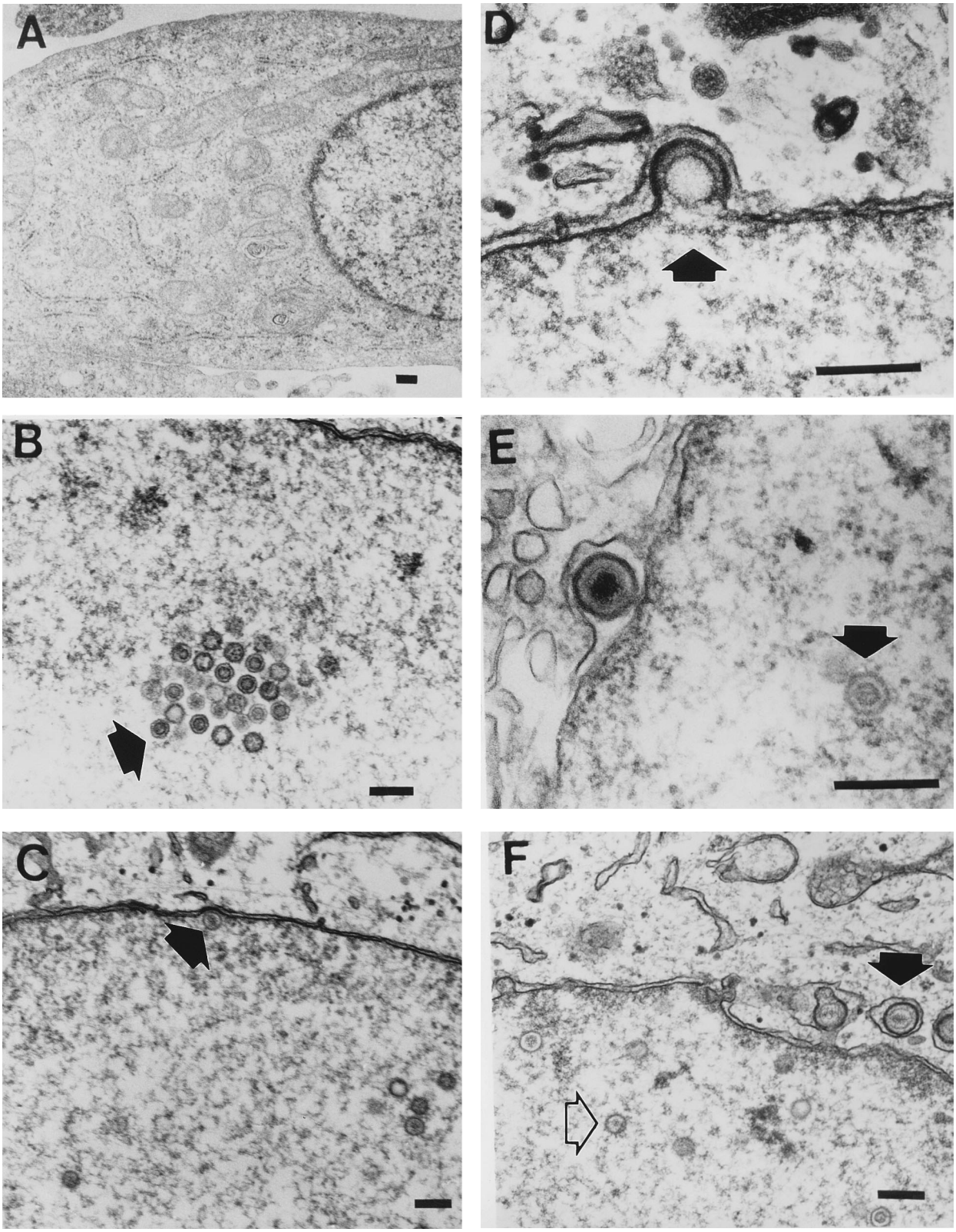

FIG. 5. Egress of viral particles from the nucleus. (A) Uninfected MeWo cell. This micrograph showed an uninfected MeWo cell with a nucleus, rough endoplasmic reticulum, and mitochondria. Bar, 200 nm in all micrographs. (B) VZV-infected cell. At 50 h postinfection VZV nucleocapsids were present in a crystalline array inside the nucleus of an infected cell (arrowhead). (C) VZV-infected cell. This nucleus of a VZV-infected MeWo cell included several nucleocapsids. One nucleocapsid lay adjacent to the nuclear membrane and appeared to be in the initial stage of envelopment (arrowhead). (D) Nucleocapsid budding through the inner nuclear membrane. The area where the nucleocapsid was adherent to the inner nuclear membrane was more electron dense. The outer nuclear membrane was clearly seen (arrowhead). (E) Nucleocapsid between the inner and outer nuclear membranes. The particle was clearly distinguishable from the nucleocapsids present within the nucleus, in that it had acquired an envelope. Note also the difference in size between the particle within the membrane and the particle still within the nucleus (arrowhead). (F) Exit of particles from nucleus. Viral particles have moved beyond the nuclear membrane into the SER. Again, note the difference in size between particles in the ER (black arrowhead) and those still in the nucleus (open arrowhead).

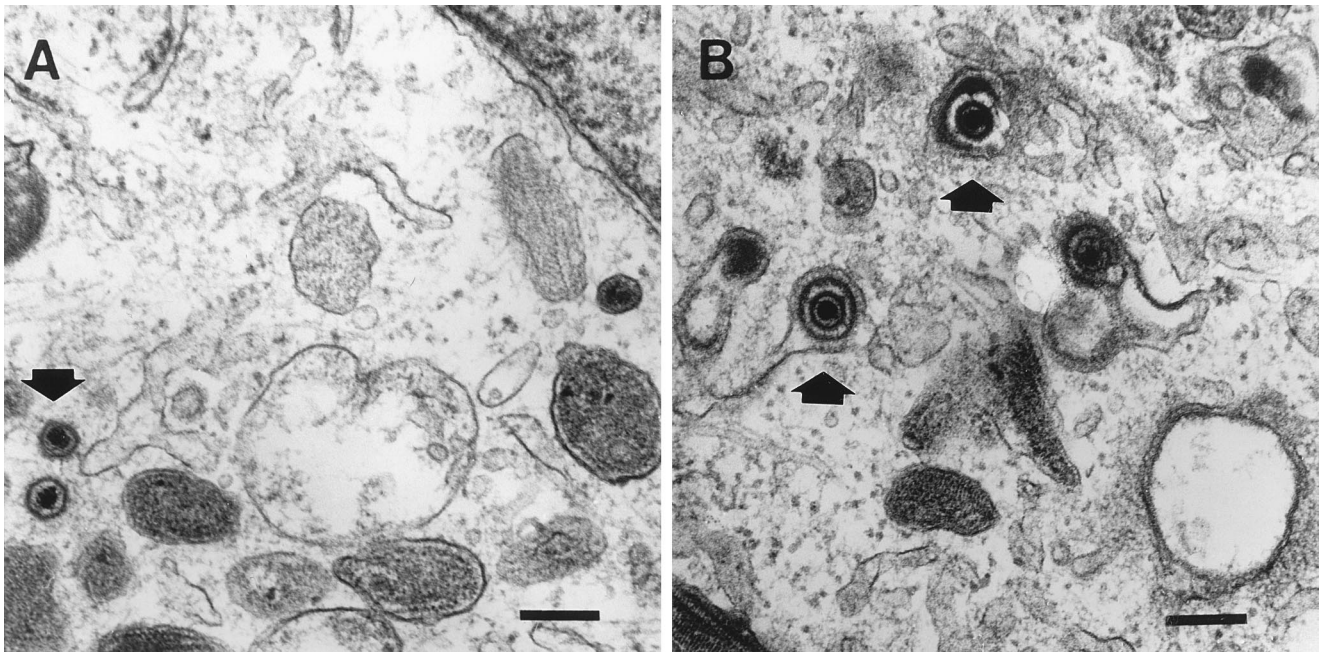

FIG. 6. Nucleocapsids in the cytoplasm. (A) Naked nucleocapsids were present within the cytoplasm of a VZV-infected MeWo cell. The nucleocapsid was 100 nm in diameter, which was one-half the diameter of the viral particles in panel B. The nucleocapsids may have lost the envelope they received while budding through the inner nuclear membrane. These naked nucleocapsids were found only on rare occasions during late infection (arrowhead). Bar, 200 nm. (B) Enveloped viral particles (arrowheads) were detected inside vacuoles within the cytoplasm of this VZV-infected MeWo cell. The diameter of an enveloped particle was 150 to 200 nm. Bar, 200 nm.

the viral particles were contained in vesicles derived from the SER is that the membranes did not contain ribosomes and, at this magnification and resolution, ribosomes would be evident. Again, these experiments were carried out five times.

Nucleocapsids in the cytoplasm. Naked nucleocapsids were seen in perinuclear areas within the cytoplasm but only in late infection and on very rare occasion. Three naked viral particles are illustrated in Fig. 6A. The two viral particles in the lower left corner have electron-dense cores and lack an envelope. A nucleus is evident in the upper right corner of the micrograph. Premelanosomes also are present. The premelanosomes appeared as vacuoles with a reticulated interior. Several segments of double endoplasmic reticulum (DER) were also located within the cytoplasm (4). In contrast to the paucity of naked nucleocapsids, viral particles within vacuoles were easily detected in the cytoplasm. At least three examples of particles within vacuoles can be seen in Fig. 6B. They were enveloped and located within membranes of the SER. Premelanosomes were easily seen. The premelanosomes were located below and to the left of the viral particles. A large vacuole with a double membrane was located just above the scale bar. There were obvious differences in size and composition of the viral particles in panels A and B.

Enveloped viral particles in an infected cell. Enveloped virions were commonplace in the VZV-infected cell at 3 days postinfection. In one exemplary micrograph, more than 150 viral particles were detected within an infected cell (Fig. 7). Enveloped viral particles were present within cytoplasmic vacuoles; most vacuoles contained one to four viral particles on cross section. Thus, each vacuole may contain up to six particles. The surface of the cell was lined with egressed viral particles. The plasma membrane often appeared discontinuous because of the numerous sites of viral egress. In the upper region of the micrograph, a vacuole was seen fusing with the plasma membrane. Of importance, the majority of the vacuoles had a single limiting membrane. Rarely was a vacuole seen with a double limiting membrane (Fig. 7, upper right corner). Several mitochondria were observed throughout the cytoplasm, as well as DER. Golgi were scarce in this micrograph. When multiple electron micrographs were examined, we calculated that about 75% of the viral particles had a dense core which indicated an intact viral genome.

Vacuoles in the cytoplasm. Although cytoplasmic vacuoles were a prominent feature of VZV-infected cells, these large vacuoles were not seen in the cytoplasm of uninfected MeWo cells. The micrograph in Fig. 8A represents a higher magnification of a vacuole illustrated in Fig. 7. The vacuole in the center of Fig. 8A was approximately 500 nm in diameter. The vacuolar membrane was a single lipid bilayer and was continuous with the plasma membrane. The large vacuole in this cross section contained four viral particles, each about 180 nm in diameter. The vacuole may have contained more than four particles, but this micrograph included only a 0.1-μm section through the vacuole. One additional viral particle was present on the surface of the plasma membrane. Two of the viral particles in the vacuole as well as the surface particle were sectioned through the core. All three had a dense core consistent with an internalized viral genome. The other two viral particles in the vacuole were sectioned through portions of the electron-dense envelope, so they appeared black. The vacuole appeared to be connected to the plasma membrane at the site of extrusion of a virion. An electron-lucent area separated the interface between the viral particle and the membrane to which it was attached. The micrograph also illustrated several mitochondria and DER characteristic of melanoma cells.

Vacuoles with reduplicated membranes were seen on rare occasion. This unusual form of the cytoplasmic vacuole is illustrated in Fig. 8B. The vacuole was 650 nm long and 400 nm at its widest point. The vacuole was only 180 nm wide in the area where two viral particles were found. Each viral particle

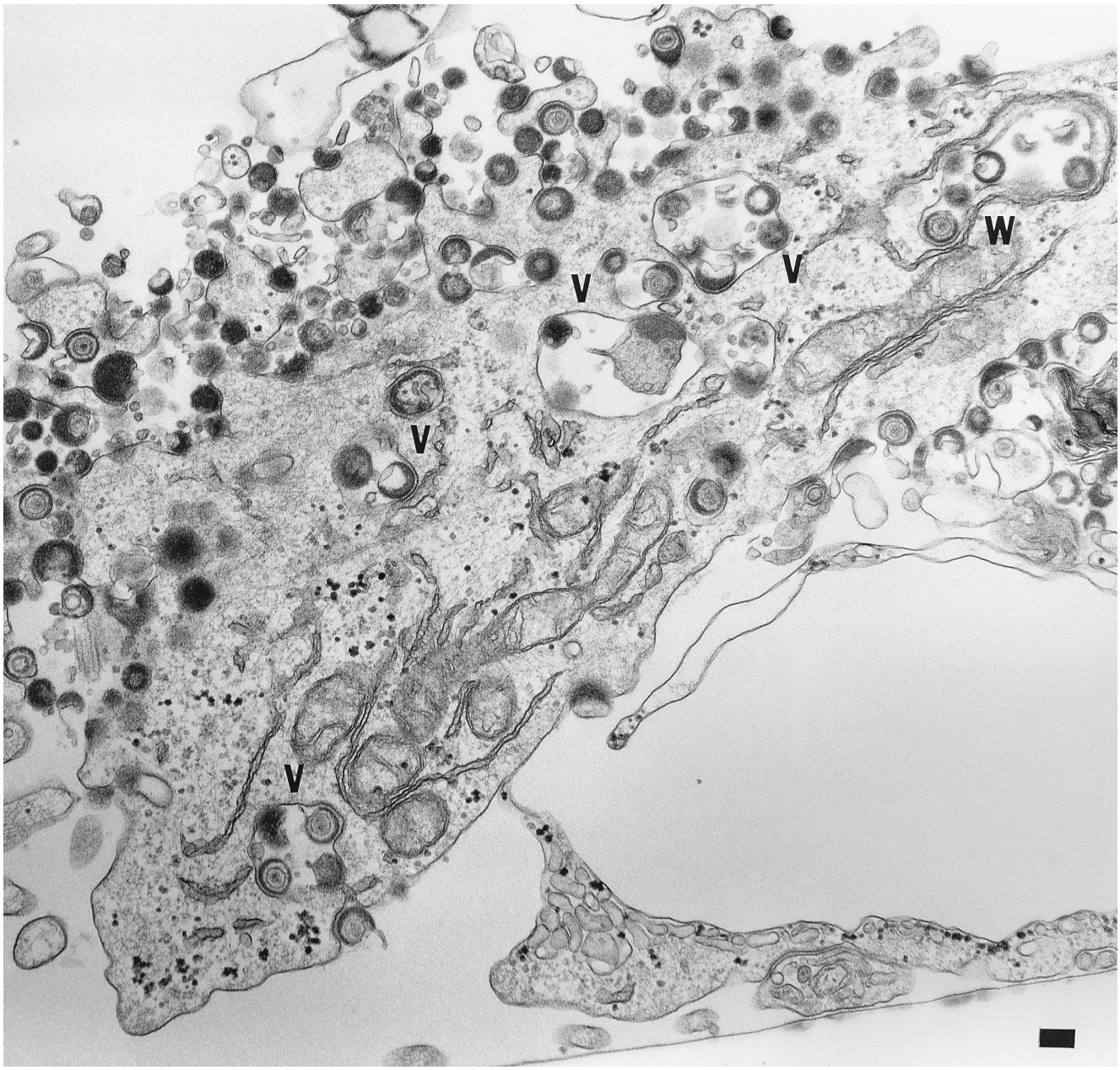

FIG. 7. Virions on the surface of the cell. Transmission electron micrograph of VZV-infected monolayer in late stages on infection. Enveloped viral particles were seen within cytoplasmic vacuoles as well as on the surface of the monolayer. Viral vacuoles had two configurations. The most common type of vacuole was surrounded by a single membrane bilayer (V). In the second type, the viral particles within a vacuole were surrounded in turn by a second membrane, a vacuole-within-a-vacuole (W). Viral particles emerging from the infected cell appeared to be surrounded by only a single membrane. Bar, 200 nm.

was 160 nm in diameter, and the particle on the left contained an electron-dense core. The phenomenon of membrane reduplication has been well documented within herpesvirus-infected cells and was thought to be a result of fusion between adjacent membranes as a result of the saturation of fusion glycoproteins found in these membranes (22, 23). It is likely that this vacuole was in contact with a segment of DER.

Enveloped viral particles and vacuoles within the nucleus. Very unexpectedly, enveloped particles were observed within the nuclei of infected cells at the latest times postinfection, when the cells were beginning to detach from the plastic surface. From the studies described above, we have speculated that nucleocapsids received their envelope as they budded through the inner nuclear membrane. While residing in the perinuclear space, some particles appeared to travel back through the inner nuclear membrane and form a vacuole composed of a membrane derived from the inner nuclear membrane. An infected cell containing intranuclear vacuoles is shown in Fig. 9. Generally, the vacuoles within the nucleus were distributed along the nuclear membrane. There were also free nucleocapsids present within the nucleoplasm. The large vacuole in this micrograph was 600 by 400 nm. It contained eight viral particles in cross section, and five of them had electron-dense cores. The others were not cross-sectioned

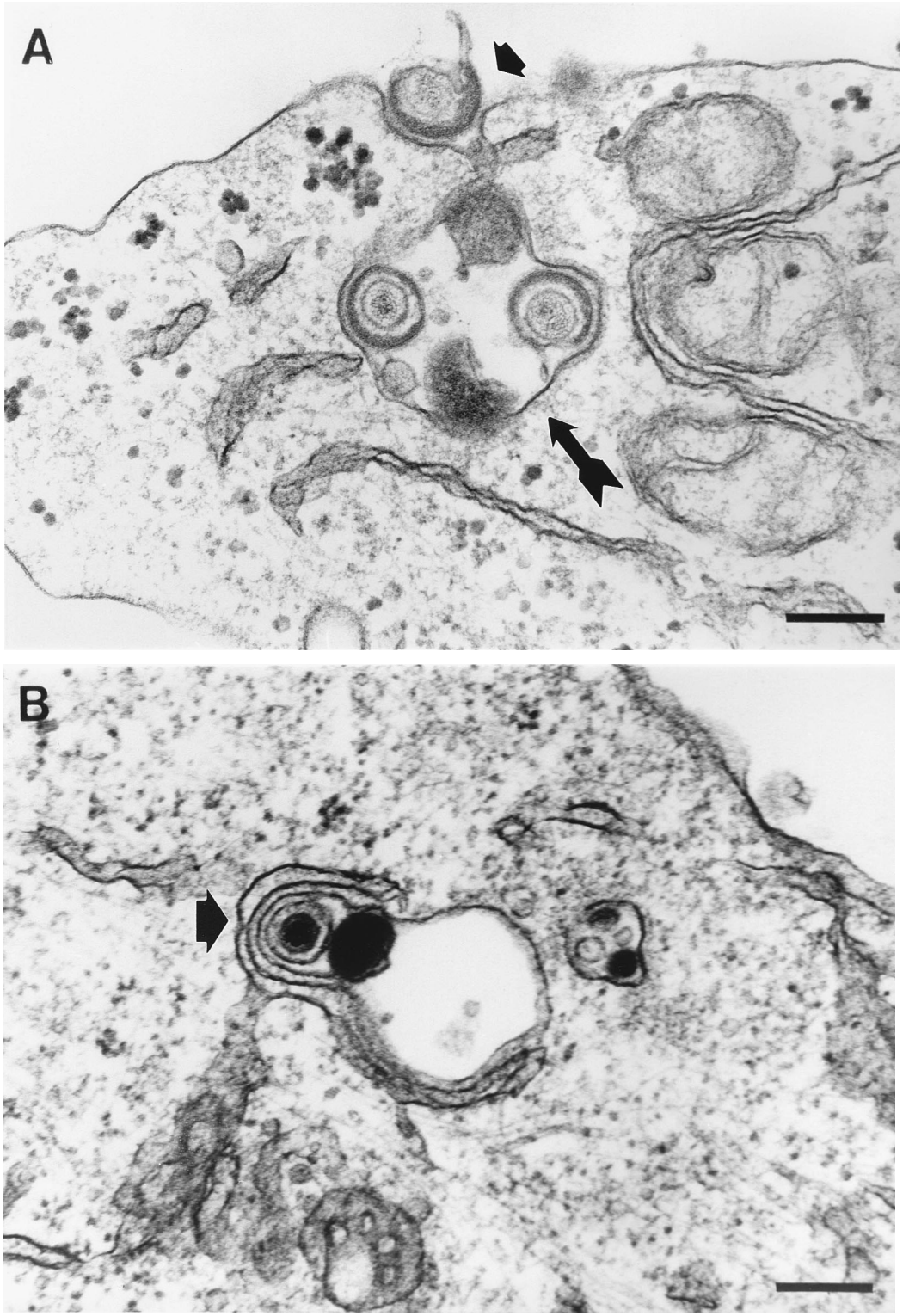

FIG. 8. Cytoplasmic vacuoles containing virions. (A) Complete enveloped virions were observed inside vacuoles (arrow) within the cytoplasm. Another virion was detected at the cell surface (arrowhead). The cytoplasmic vacuole appeared to be connected to the indented cell membrane containing the emergent viral particle. Thus, the particle at the cell surface may represent the final stage of egress. Bar, 200 nm. (B) Vacuole containing enveloped virions. The vacuole was contiguous with a semicircular membranous structure which most likely represented a portion of DER (arrowhead). The pattern of reduplicated membranes was an unusual phenomenon in VZV-infected melanoma cells. Bar, 200 nm.

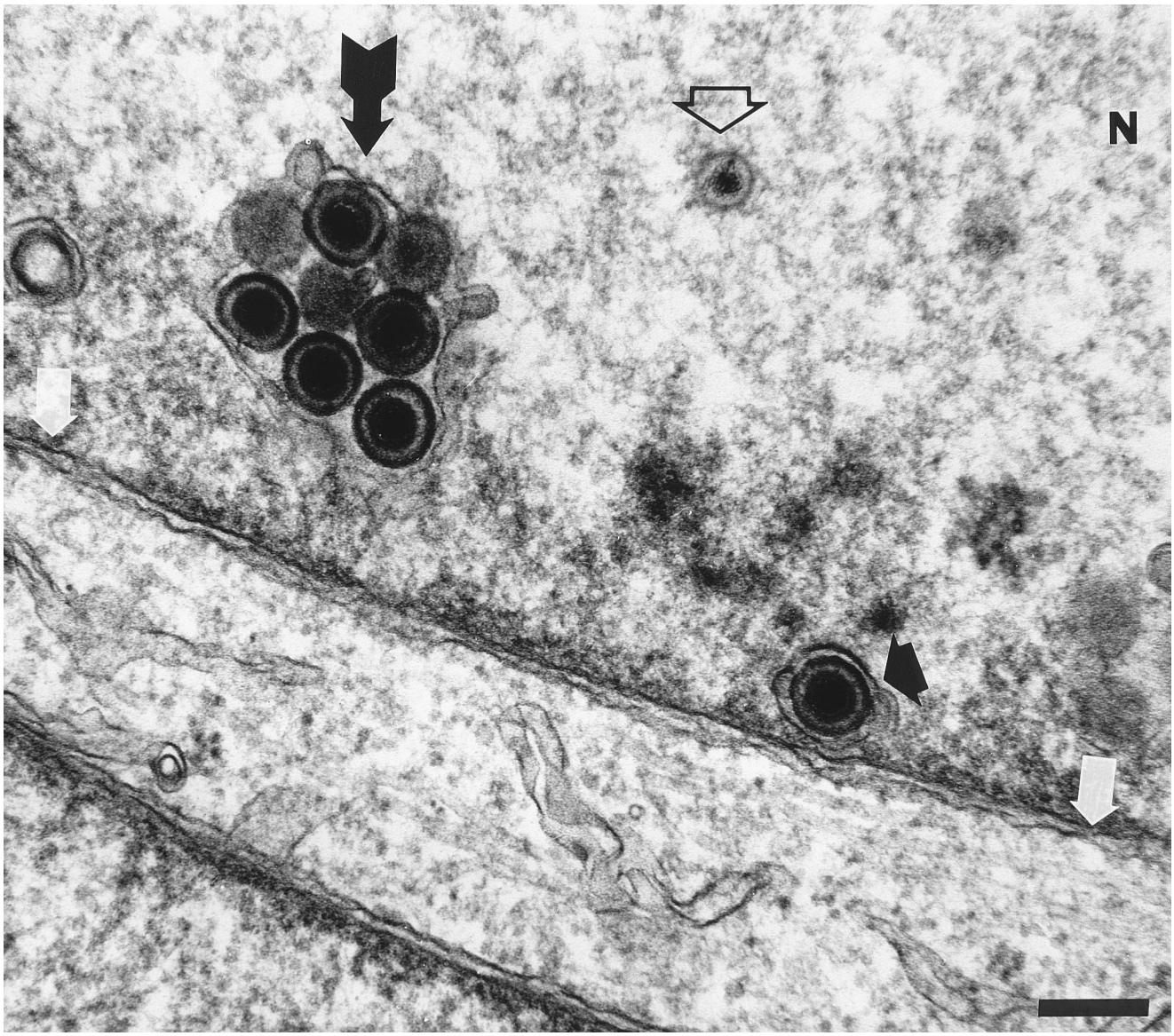

FIG. 9. Enveloped viral particles in nucleoplasm (N). A large vacuole contained a cluster of at least eight enveloped virions (arrow). The enveloped viral particle adjacent to the nuclear membrane (white arrows) may have reentered the nucleoplasm by budding through the inner nuclear membrane (arrowhead). A few naked nucleocapsids also were present within the nucleoplasm (open arrowhead). Bar, 200 nm.

through the center. Two other vacuoles contained only one viral particle apiece. There was also a free nucleocapsid in the nucleoplasm that was unenveloped and had an electron-dense core. The two nuclei in this micrograph were not separated by a plasma membrane.

Some nuclear vacuoles contained mainly enveloped viral particles, whereas other vacuoles contained an assortment of enveloped and unenveloped particles, as well as vacuoles within vacuoles. The large vacuole in Fig. 10 is an example of the latter phenomenon. It measured 600 by 900 nm. The larger vacuole contained single enveloped particles as well as at least three smaller vacuoles, each of which contained one or two nonenveloped particles. Most of the viral particles appeared to have dense cores. The particles ranged in size from 100 to 200 nm. The interface between the prominent enveloped particles within the large vacuole and the adjacent vacuolar membrane was very noticeable because the vacuole membrane appeared more electron dense. The vacuoles were visualized in multiple TEM sections through the nucleus; therefore, they could not represent a chance occurrence of a vacuole within an invagination of cytoplasm into the nucleus.

VZV infection of human diploid lung cells. Upon completion of the preceding examination of VZV-infected human melanoma cells, we repeated the TEM analysis in VZV-infected cultures of MRC-5 human diploid lung cells. After comparing the micrographs, we concluded that VZV infection of human fetal lung cells was more aberrant (Fig. 11). The criteria included the following: (i) there was a lower percentage of virions containing nucleocapsids, and (ii) the human diploid cell substrate itself appeared more disrupted with microfibril formation and very large cytoplasmic vacuoles. In VZV-infected melanoma cells, most of the cytoplasmic vacuoles contained (in cross section) between one and four virions; the virions themselves usually contained a nucleocapsid. In VZV-

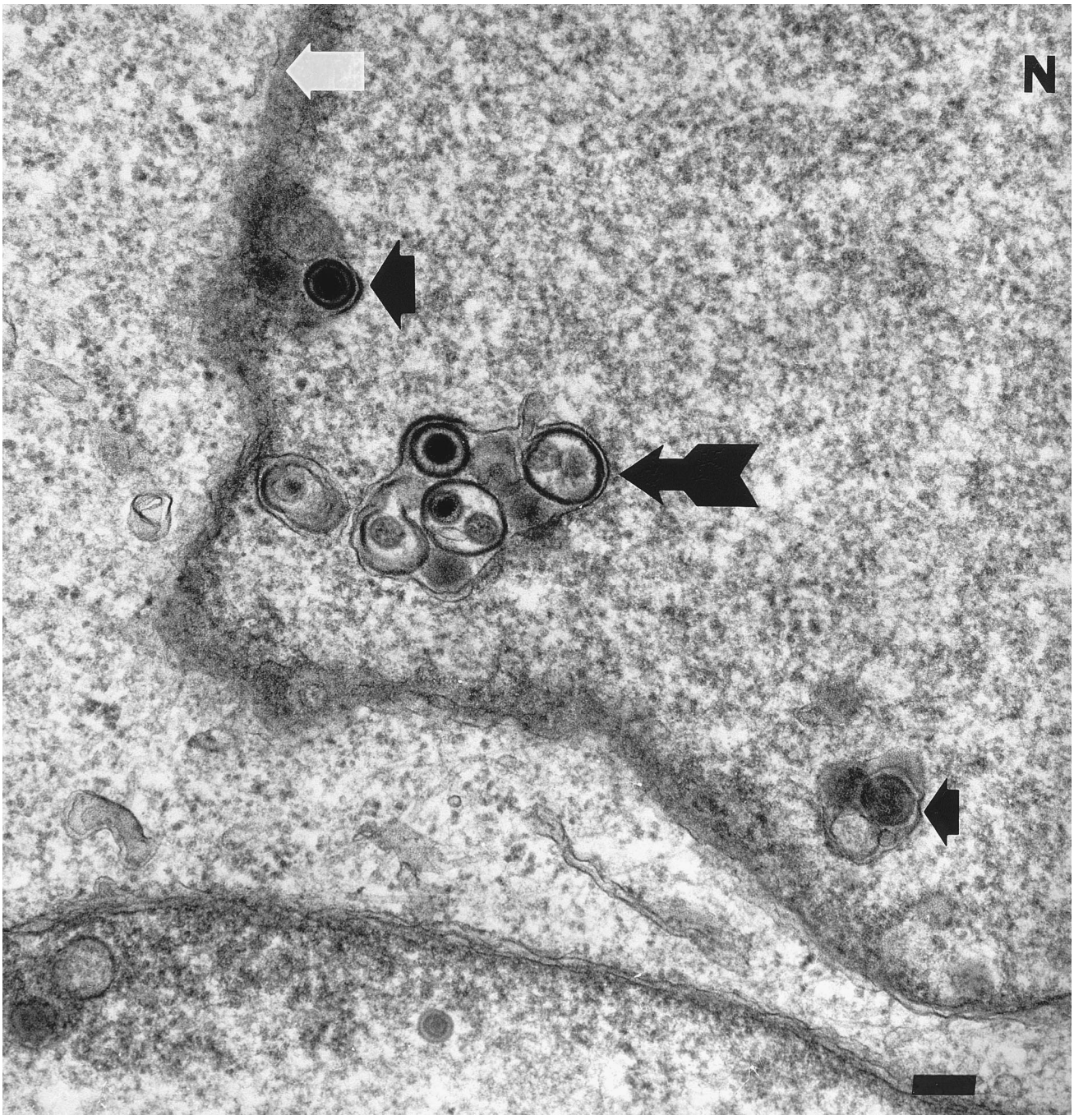

FIG. 10. Vacuoles-within-a vacuole within the nucleoplasm (N). The nuclear membrane was clearly visible (white arrow). One prominent intranuclear vacuole which contained three smaller vacuoles was observed (black arrow). Each of the smaller vacuoles contained one or two naked nucleocapsids, while at least one enveloped particle was observed within the larger vacuole but not within any of the smaller vacuoles. Another enveloped viral particle appeared at an indentation of the inner nuclear membrane and may represent a particle reentering the nucleus (larger black arrowhead). Another vacuole also was observed in the nucleus (smaller black arrowhead). Bar, 200 nm.

infected lung cells, the vacuoles were considerably larger and were rimmed with viral particles; on higher magnification, a majority of the particles were found to have only an envelope-like structure but no nucleocapsid. The latter cells also contained numerous lysosome bodies. A comparison of all the micrographs in this article suggests that there may be more lysosomes in VZV-infected fetal diploid lung cells.

DISCUSSION

This discussion is based on the hypothesis that the melanocyte is a preferred cell substrate for replication of VZV. Because of the difficulties with isolation and culture of the primary human melanocyte, we have examined a human melanoma cell line designated MeWo (12, 13). Even though

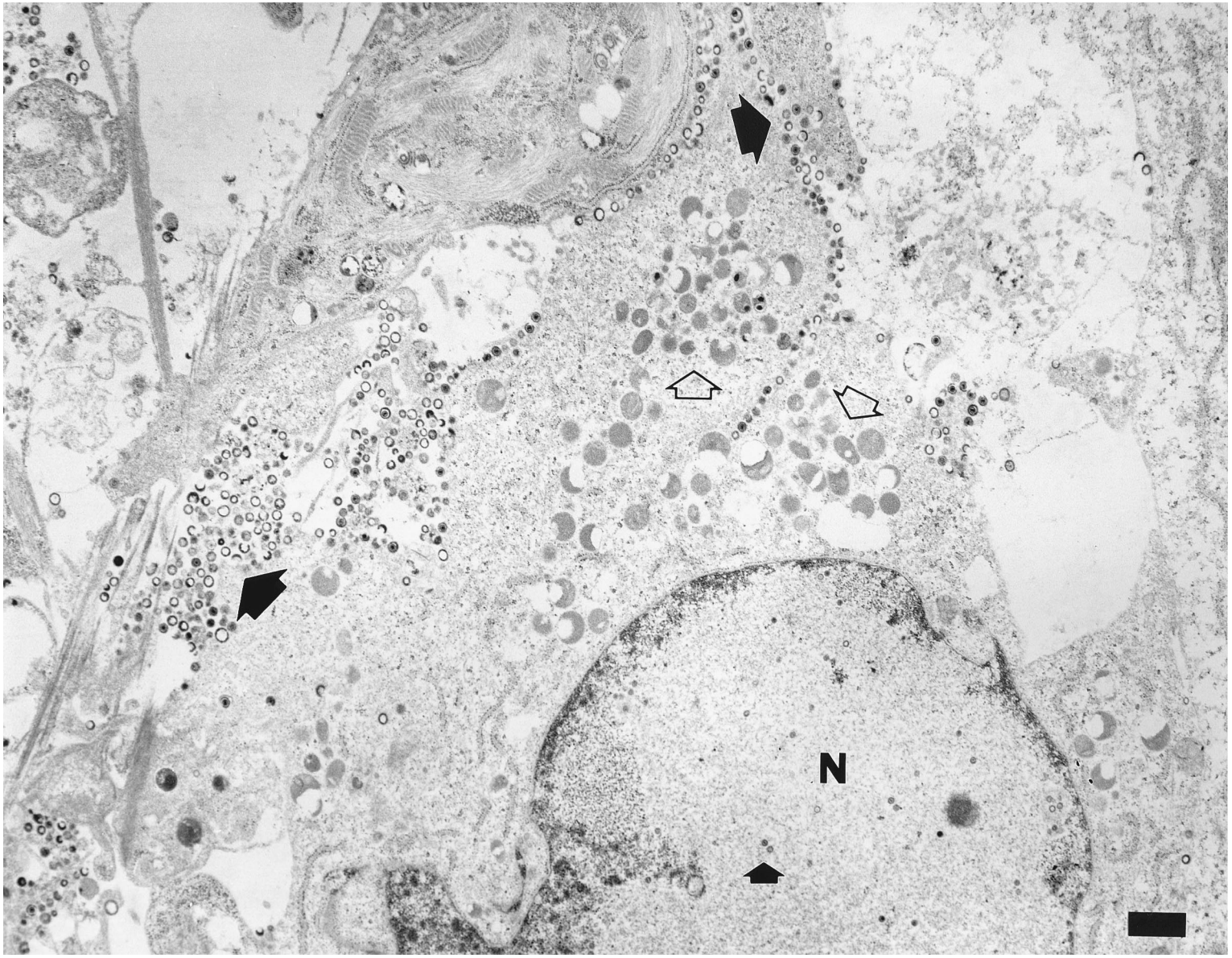

FIG. 11. Human fetal diploid lung cells infected with VZV-32. Human fetal diploid lung cells infected with VZV-32 were processed for examination by TEM at 3 days postinfection, when cytopathology was advanced. A nucleus visible in the lower portion of the micrograph (N) contained several nucleocapsids (small black arrowhead). Many lysosomes were present in the perinuclear areas. The lysosomes appeared as circular or crescent-shaped structures (open arrowheads). Scores of viral particles were located along the surface of the plasma membrane or at the junction between cells (larger black arrowheads). A majority of the cytoplasmic particles did not contain a nucleocapsid; rather they appeared to be only an outer envelope structure. Some of the particles were housed within large vacuolar structures. Large vacuoles were observed in the cytoplasm of the infected cells. Bar, 1 μm.

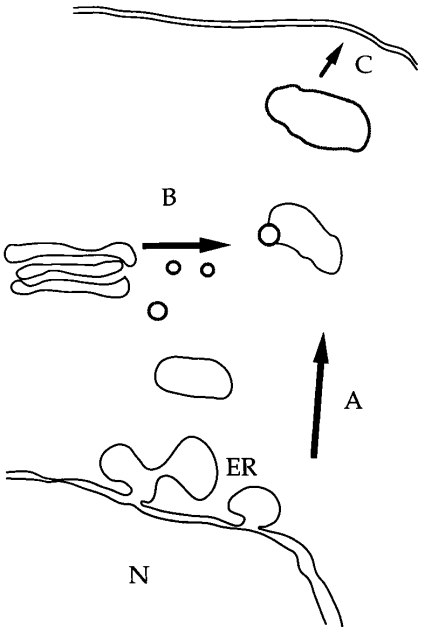

FIG. 12. Melanogenesis. (A) A premelanosome is formed by a pinching-off process from the SER. N, nucleus. (B) Tyrosinase, an enzyme that catalyzes the formation of melanin within the melanosome, is glycosylated within the Golgi apparatus and then transported to the premelanosome within Golgi-derived vesicles. These vesicles fuse with the premelanosome and release the enzyme in order to form the mature melanosome. (C) The melanosome travels through the dendrites of the melanocyte into the neighboring keratinocyte, where the melanosome releases melanin into the cytoplasm of the cell. This pathway is based on data contained in references 4, 15, and 19.

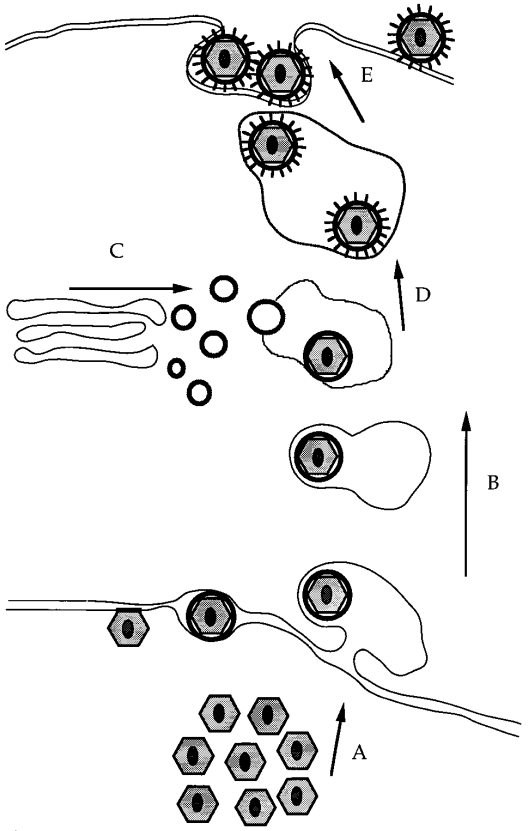

FIG. 13. Schema for envelopment and egress of VZV particles. (A) Nucleocapsids within the nucleoplasm bud through the inner nuclear membrane and acquire an envelope. They travel through the perinuclear space into the SER. (B) The SER vacuole is pinched off and enters the cytoplasm. (C) Vesicles from the Golgi containing VZV glycoproteins travel to and fuse with the SER-derived vacuole containing nascent virions. (D) Virion-laden vesicles fuse with one another to form a larger vacuole containing two to four complete viral particles. (E) Vacuoles fuse with the plasma membrane, and enveloped virions emerge on the surface of the infected cell. This schema includes data from reference 16.

the melanoma cell is the malignant counterpart of the melanocyte, it usually retains the ability to produce melanin; in some cases, melanoma cells are actually overproducers of melanin (15, 19). The VZV hypothesis is expanded to include the observation that VZV usurps the cell machinery for melanin production in order to assemble the VZV virion. To briefly summarize, the production of melanin is carried out in two stages. In one stage, the melanosome is formed by a pinching-off process from the SER within the melanocyte or melanoma cell; at this early stage the nascent vacuole is called the premelanosome (19). The vacuole contains the framework on which melanin will be formed, but it does not yet include the essential enzyme tyrosinase. The enzyme tyrosinase catalyzes the conversion of the amino acid tyrosine to dopa. Dopa is then converted to dopaquinone and other intermediary compounds before the emergence of the end product melanin. Of importance with regard to the hypotheses regarding VZV assembly, tyrosinase is not present within the premelanosome (15). Rather it is a traditional glycoprotein which first enters the ER but is subsequently transferred to the Golgi for processing and sialation of its N-linked oligosaccharides (24). From the Golgi, the enzyme exits in transport vesicles which travel to and fuse with the premelanosome (19). Only after this event occurs, can melanin be produced within the melanosome. The melanosome in turn is transported via dendrites of the melanocyte into the adjacent keratinocytes. Within the keratinocytes, the melanosome releases its skin pigment. A simplified pathway is shown in Fig. 12.

As part of the VZV assembly hypothesis, we propose the following scenario. The nucleocapsid passes through the inner nuclear membrane and acquires its initial envelope. The enveloped particle travels through the perinuclear space where it is engulfed within a vacuole formed in a similar manner to the premelanosome. A vacuole containing one or more viral particles is pinched off and resides within the cytoplasm. After the viral glycoproteins are formed during transit in the Golgi, they collect within transport vesicles, in a manner similar to tyrosinase, and travel to and fuse with an SER vacuole containing viral particles. Once viral glycoproteins, including the VZV fusogen gH-gL complex, have entered the vacuole, the vacuole can fuse with one or more neighboring vacuoles to form a larger vacuole containing two to four viral particles. In turn, the vacuole exhibits the exocytic properties of a melanosome, whereby it can travel through the cytoplasm and fuse with the outer cell membrane. A proposed pathway of VZV egress with its similarity to melanogenesis is shown in Fig. 13. Furthermore, a pathway for the retrograde movement of particles into the nucleus during late infection is illustrated in Fig. 14. The enveloped virions within the nucleus presumably received their envelope from the inner nuclear membrane during their earlier egress. In addition, nucleocapsids still resident in the nucleus presumably recognized the vacuolar membrane as an inner nuclear membrane and thereby budded into the nuclear vacuole. Thus, by error, nucleocapsids entered nuclear vacuoles without ever passing into the perinuclear space.

What other similarities exist between a melanosome vacuole and the VZV vacuole? Glycoproteins other than tyrosinase are

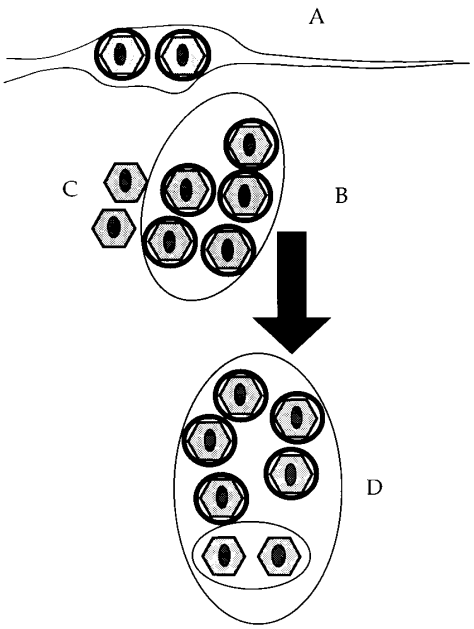

FIG. 14. Schema for retrograde transport to nucleus. (A) Two enveloped viral particles are portrayed between the inner and the outer nuclear membrane. When they exhibit retrograde flow, they reenter the nucleus within a vacuole derived from the inner nuclear membrane. (B) Vacuoles containing enveloped particles are found in the nucleoplasm. (C) Naked nucleocapsids within the nucleus recognize the membrane of a vacuole as inner nuclear membrane and adhere to it. (D) Vacuoles sometimes contain viral particles from the perinuclear space as well as viral particles which have entered directly from the nucleus. Thus, a vacuole-within-a-vacuole is formed within the nucleus of an infected cell.

transported from the Golgi to the melanosome. In addition, these same glycoproteins are transported to the outer cell membrane directly. Thus, both the melanosome and the outer cell membrane of the melanocyte contain distinctive glycoproteins (15, 19). Likewise, a long-observed but little-understood observation in VZV-infected cells is that viral glycoproteins can be detected on the surfaces of infected cells before the appearance of progeny virions (17). The melanosome model provides another example of this phenomenon (19, 30). Furthermore, monensin treatment of melanoma cells induces a selective loss of melanin deposition in premelanosomes; the premelanosomes were markedly enlarged, with a vacant interior (19). Monensin treatment of VZV-infected cells also inhibits the formation of enveloped virions (20).

Further data in support of the melanosome hypothesis were provided in earlier studies from this laboratory. Montalvo et al. (21) applied the periodate-thiocarbohydrazide silver proteinate (PA-TCH-SP) method to the study of VZV envelopment. Staining by the PA-TCH-SP method, which localizes glycoconjugates within a cell, is represented by silver grains. Montalvo et al. (21) were unable to demonstrate the presence of glycoconjugates within the nucleus or the inner nuclear membrane of VZV-infected MeWo cells, while moderate staining was observed in the Golgi cisternae. Likewise, enveloped virions within cytoplasmic vacuoles stained PA-TCH-SP positive, and periodate-reactive glycoconjugates were located on the inside of the vacuolar membrane. This localization is compatible with the expected appearance of the N terminus of type 1 glycoproteins inside of a cytoplasmic vacuole. When Montalvo et al. (20) added either of two inhibitors of glycosylation, monensin and tunicamycin, to VZV-infected MeWo cells, they demonstrated that the maturation of VZV glycoprotein gE could be blocked. The latter study reaffirms the ER-Golgi as the site of viral glycoprotein processing and the cytoplasmic vacuole as the site of virion envelope maturation.

Subsequently, Jones and Grose (16) studied the assembly of VZV virions and the formation of cytoplasmic vacuoles by a combination of TEM, pulse-chase analysis, autoradiography, and cross-fire probability matrix analysis to identify individual subcellular compartments. Since VZV infection shuts off host cell glycoprotein synthesis by the cell substrate, virtually all fucosylated proteins are of viral origin and include the three major VZV glycoproteins gE, gB, and gH (10). Thus, fucose is an ideal marker by which to study the trafficking of mature viral glycoproteins. In this detailed study, the delineated pathway for the fucosylated glycoproteins led from the Golgi to virion-laden cytoplasmic vacuoles to the regions of the outer cell membrane associated with emergent virions. Of importance, there was no evidence for a retrograde movement of fucosylated VZV proteins from the Golgi back to the nuclear membrane. Thus, the above data are wholly compatible with the melanosome model, in which the viral glycoproteins behaving like tyrosinase bud from the Golgi in transport vesicles which travel to and fuse with a vacuole derived from the SER.

Is there additional evidence for the role of melanocytes? It is now established that VZV pathogenesis follows a viremia model (11). Therefore, virus must pass from the capillaries into the skin in order to form the characteristic rash. Numerous studies over the years have established that VZV multiplication does not occur within the dermis but at the basal layer of the epidermis, a site where melanocytes are concentrated. In addition, melanocytes are also located at the base of the hair follicle. Biopsy studies of children with chickenpox have shown an abundance of viral proteins in the basal layer and stratum malpighi of the epidermis, including the hair follicle (34). On the basis of the melanosome model, vacuoles containing VZV would exit the melanocyte and expell their virions within the keratinocytes.

VZV envelopment has also been studied in great detail by Gershon et al. (8, 9). They propagated a higher-passage VZV-Ellen strain in human embryo lung fibroblast (HELF) cultures. Not all conclusions from their reports and our reports are the same, but in this case we ascribe most of the differences to the cell substrate. They observed a process which has been called envelopment, deenvelopment, and reenvelopment (9, 36). As reviewed in the above paragraphs, we concur with their conclusion that the initial viral envelope acquired at the inner nuclear membrane does not contain VZV glycoproteins, certainly not VZV glycoprotein gE. Likewise, we concur that the viral glycoproteins are initially processed and transported from the ER to the Golgi independently of the pathway for virus assembly. However, after examination of more than 200 electron micrographs taken at increasing intervals postinfection during five time-course experiments, we failed to find evidence for deenvelopment and reenvelopment. More specifically, we searched at great length in our cell system but did not find what they described as VZV-associated sacs that appeared to provide the final envelope for nucleocapsids within the cytosol of VZV-infected HELF cultures (9). Instead, we found that greater than 95% of all detectable viral particles were housed in vacuoles; more than 75% of these particles were normal in appearance with an electron-dense core and a single complete envelope.

Because of these obvious differences between VZV-32-infected MeWo cells and VZV-Ellen-infected HELF cells, we infected a lung diploid cell line called MRC-5 and repeated the TEM examination. We observed many of the viral morphological features described by Gershon et al. (9); in particular, we

noted that the entire assembly and envelopment process was more aberrant in MRC-5 cells, including an increased number of nucleocapsids in the cytoplasm as well as considerable heterogeneity in the morphology of the enveloped particles. This diversity in VZV particle structure had been carefully documented earlier by Nii (22), an investigator who used a VZV-Vero cell system. In addition, we observed a large number of lysosomes in VZV-infected lung cells, as previously noted by Gershon et al. (9). When infectivity titrations were carried out in human melanoma cells, the titer was about one log unit higher than that usually obtained in fibroblast cells (12). For the above reasons, we conclude that VZV envelopment is not a uniform process in all permissive cell substrates. As an extension, the broader concept that alphaherpesvirus envelopment may vary depending on the cell substrate certainly would resolve many conflicting statements in the cited articles (5, 23, 32, 36).

Finally, the melanocyte hypothesis offers a possible explanation for two other phenomena: (i) hypopigmentation associated with congenital varicella infection and (ii) replication of MDV in the feather follicle. With regard to point i, congenital varicella syndrome occurs in a small number of fetuses who are infected as a consequence of maternal gestational chickenpox (29). A major feature of the syndrome is cutaneous zig-zag scarring, also called a cicatrix. The skin surrounding a cicatrix often is hypopigmented, presumably as a result of viral disruption of the migrating neural crest cells, which then fail to become melanocytes within the involved epidermis. With regard to point ii, MDV is an oncogenic avian virus which was originally classified as a gammaherpesvirus. However, the unique short region of the MDV viral genome is more similar to that of alphaherpesviruses such as VZV (2). Although the virus can be propagated in vitro in chicken embryo cultures (6), early work has shown that the primary site of MDV envelopment in vivo is within the feather follicle epithelia of infected chickens (3). Melanocytes are not common in the body skin of most breeds of chickens but are prevalent within the feather follicle (1, 18). Thus, avian melanocytes may be a preferred cell substrate for the MDV lytic replication cycle.

ACKNOWLEDGMENT

This research was supported by USPHS grant AI 22795.

REFERENCES

1. **Bowers, R. R.** 1988. The melanocyte of the chicken: a review, p. 49–63. *In* J. T. Bagnara (ed.), Advances in pigment cell research: progress in clinical and biological research, vol. 256. Alan R. Liss, Inc., New York.
2. **Brunovskis, P., L. F. Velicer.** 1995. The Marek's disease virus (MDV) unique short region: alphaherpesvirus-homologous, fowlpox virus-homologous, and MDV-specific genes. Virology **206:**324–338.
3. **Calnek, B. W., H. K. Adldinger, and D. E. Kahn.** 1970. Feather follicle epithelium: a source of enveloped and infectious cell-free herpesvirus from Marek's disease. Avian Dis. **14:**219–233.
4. **Chang, J. P., T. Saito, M. M. Romsdahl, and W. O. Russell.** 1969. Electron microscopy of human melanoma tissues and cells during mitosis, p. 51–70. *In* V. Riley (ed.), Pigmentation: its genesis and biological control. Appleton-Century-Crofts, Meredith Corporation, New York.
5. **Cheung, P., B. W. Banfield, and F. Tufaro.** 1991. Brefeldin A arrests the maturation and egress of herpes simplex virus particles during infection. J. Virol. **65:**1893–1904.
6. **Cook, M. K., and J. F. Sears.** 1970. Preparation of infectious cell-free herpestype virus associated with Marek's disease. J. Virol. **5:**258–261.
7. **Davison, A. J., and J. E. Scott.** 1986. The complete DNA sequence of varicella-zoster virus. J. Gen. Virol. **67:**1759–1816.
8. **Gershon, A., L. Cosio, and P. A. Brunell.** 1973. Observations on the growth of varicella-zoster virus in human diploid cells. J. Gen. Virol. **18:**21–31.
9. **Gershon, A. A., D. L. Sherman, Z. Zhu, C. A. Gabel, R. T. Ambron, and M. D. Gershon.** 1994. Intracellular transport of newly synthesized varicella-zoster virus: final envelopment in the *trans*-Golgi network. J. Virol. **68:**6372–6390.
10. **Grose, C.** 1980. The synthesis of glycoproteins in human melanoma cells infected with varicella-zoster virus. Virology **101:**1–9.
11. **Grose, C.** 1981. Variation on a theme by Fenner: the pathogenesis of chickenpox. Pediatrics **68:**735–737.
12. **Grose, C., and P. A. Brunell.** 1978. Varicella-zoster virus: isolation and propagation in human melanoma cells at 36 and 32°C. Infect. Immun. **19:**199–203.
13. **Grose, C., D. M. Perrotta, P. A. Brunell, and G. C. Smith.** 1979. Cell-free varicella-zoster virus in cultured melanoma cells. J. Gen. Virol. **43:**15–27.
14. **Hayat, M. A.** 1989. Principles and techniques of electron microscopy, 3rd ed., p. 1–469. CRC Press, Inc., Boca Raton, Fla.
15. **Jimbow, K., K. Yamana, Y. Akutsu, and K. Maeda.** 1988. Nature and biosynthesis of structural matrix protein in melanosomes: melanosomal structural protein as differentiation antigen for neoplastic melanocytes, p. 169–182. *In* J. T. Bagnara (ed), Advances in pigment cell research: progress in clinical and biological research, vol. 256. Alan R. Liss, Inc., New York.
16. **Jones, F., and C. Grose.** 1988. Role of cytoplasmic vacuoles in varicella-zoster virus glycoprotein trafficking and virion envelopment. J. Virol. **62:**2701–2711.
17. **Litwin, V., M. Sandor, and C. Grose.** 1990. Cell surface expression of the varicella-zoster virus glycoproteins and Fc receptor. Virology **178:**263–272.
18. **Lucas, A. M., and P. R. Stettenheim.** 1972. Avian anatomy: integument, p. 397–401. United States Department of Agriculture, Washington, D.C.
19. **Mishima, Y., M. Ichihashi, K. Hayashibe, M. Ueda, S. Hatta, F. Yoko, and G. Imokawa.** 1988. Control of melanogenesis and melanoma oncogenesis, p. 127–141. *In* J. T. Bagnara (ed.), Advances in pigment cell research: progress in clinical and biological research, vol. 256. Alan R. Liss, Inc., New York.
20. **Montalvo, E. A., R. T. Parmley, and C. Grose.** 1985. Structural analysis of the varicella-zoster virus gp98-gp62 complex: posttranslational addition of N-linked and O-linked oligosaccharide moieties. J. Virol. **53:**761–770.
21. **Montalvo, E. A., R. T. Parmley, and C. Grose.** 1986. Varicella-zoster viral glycoprotein envelopment: ultrastructural cytochemical localization. J. Histochem. Cytochem. **34:**281–284.
22. **Nii, S.** 1973. Aberrant forms of varicella-zoster virus. Biken J. **16:**173–176.
23. **Nii, S.** 1991. Electron microscopic study on the development of herpesvirus. J. Electron Microsc. **41:**414–423.
24. **Nishioka, K.** 1978. Particulate tyrosinase of human malignant melanoma; Solubilization, purification following trypsin treatment and characterization. Eur. J. Biochem. **85:**137–146.
25. **Pawley, J. B.** 1990. Handbook of biological confocal microscopy, rev. ed., p. 1–232. Plenum Press, New York.
26. **Reynolds, E. S.** 1963. The use of lead citrate at high pH as an electron-opaque stain in electron microscopy. J. Cell Biol. **17:**208–215.
27. **Rodriguez, J. E., T. Moninger, and C. Grose.** 1993. Entry and egress of varicella virus blocked by same anti-gH monoclonal antibody. Virology **196:**840–844.
28. **Roizman, B.** 1962. Polykaryocytosis induced by viruses. Proc. Natl. Acad. Sci. USA **48:**228–234.
29. **Savage, M. O., A. Moosa, and R. R. Gordon.** 1973. Maternal varicella infection as a cause of fetal malformations. Lancet **i:**352–354.
30. **Szabó, G., A. B. Gerald, M. A. Pathak, and T. B. Fitzpatrick.** 1969. The ultrastructure of racial color differences in man, p. 23–41. *In* V. Riley (ed.), Pigmentation: its genesis and biological control. Appleton-Century-Crofts, Meredith Corporation, New York.
31. **Szilágyi, J. F., and C. Cunningham.** 1991. Identification and characterization of a novel non-infectious herpes simplex virus-related particle. J. Gen. Virol. **72:**661–668.
32. **Van Genderen, I. L., R. Brandimarti, M. R. Torrisi, G. Campadelli, and G. Van Meer.** 1994. The phosopholipid composition of extracellular herpes simplex virions differs from that of host cell nuclei. Virology **200:**831–836.
33. **Watson, M. L.** 1958. Staining of tissue sections for electron microscopy with heavy metals. J. Biophys. Biochem. Cytol. **4:**475–478.
34. **Weigle, K. A., and C. Grose.** 1983. Common expression of varicella-zoster viral glycoprotein antigens in vitro and in chickenpox and zoster vesicles. J. Infect. Dis. **148:**630–638.
35. **Weller, T. H.** 1953. Serial propagation in vitro of agents producing inclusion bodies derived from varicella and herpes zoster. Proc. Soc. Exp. Biol. Med. **83:**340–346.
36. **Whealy, M. E., J. P. Card, R. P. Meade, A. K. Robbins, and L. W. Enquist.** 1991. Effect of brefeldin A on alphaherpesvirus membrane protein glycosylation and virus egress. J. Virol. **65:**1066–1081.

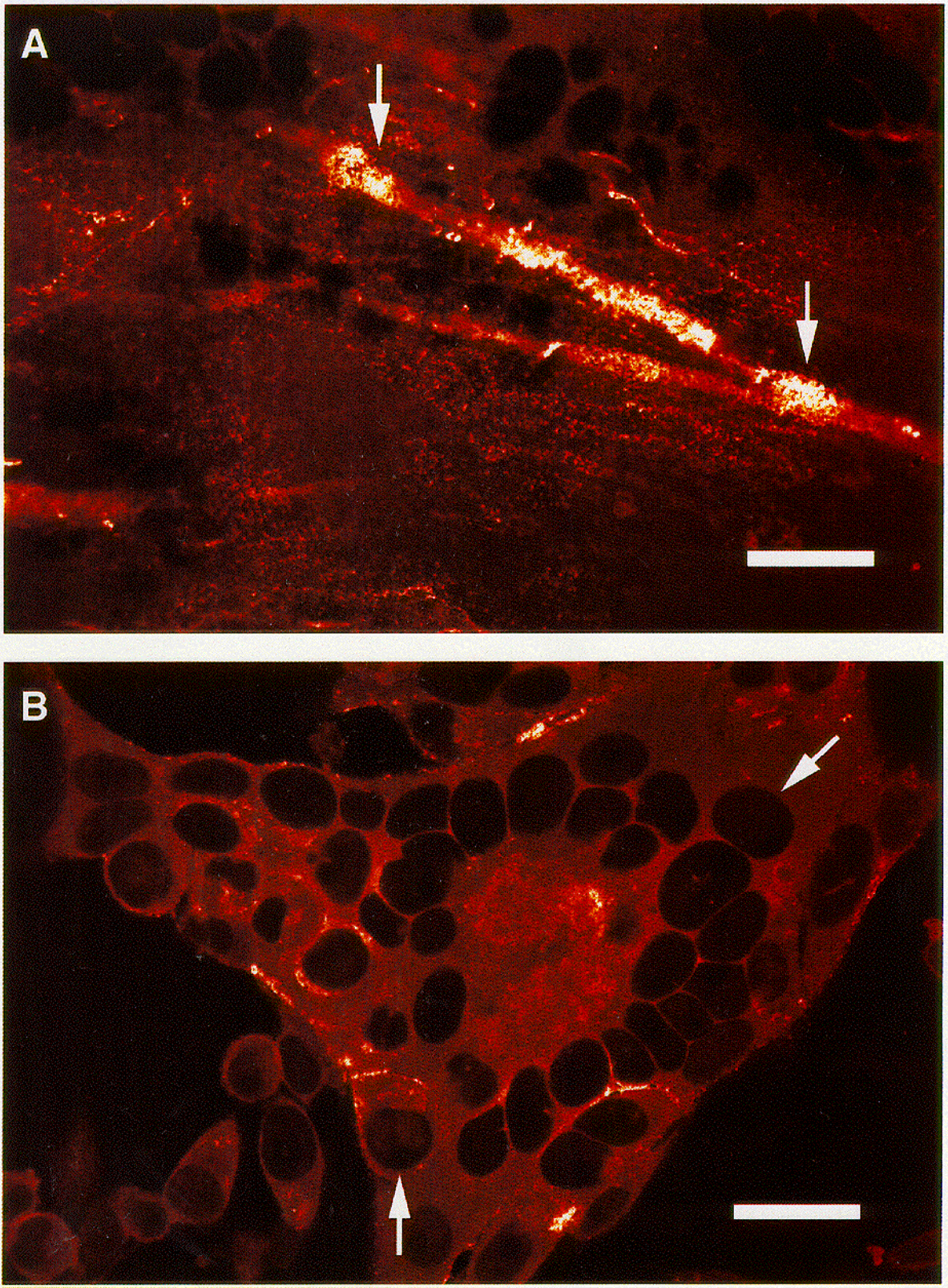
A
B